

Donor Characteristics of Transition-Metal-Doped Oxides: Cr-Doped MgO versus Mo-Doped CaO

Fernando Stavale,^{†,§} Xiang Shao,^{†,§} Niklas Nilius,^{*,†} Hans-Joachim Freund,[†] Stefano Prada,[‡] Livia Giordano,^{*,‡} and Gianfranco Pacchioni[‡]

[†]Fritz-Haber-Institut der Max-Planck-Gesellschaft, Faradayweg 4-6, D-14195 Berlin, Germany

[‡]Dipartimento di Scienza dei Materiali, Università di Milano-Bicocca, via Cozzi 53, 20125 Milano, Italy

Supporting Information

ABSTRACT: The ability of Mo (Cr) impurities in a CaO (MgO) matrix to act as charge donors to adsorbed gold has been investigated by means of scanning tunneling microscopy and density functional theory. Whereas CaO_{Mo} features a robust donor characteristic, as deduced from a charge-transfer-driven crossover in the Au particles' geometry in the presence of dopants, MgO_{Cr} is electrically inactive. The superior performance of the CaO_{Mo} system is explained by the ability of the Mo ions to evolve from a +2 oxidation state in ideal CaO to a +5 state by transferring up to three electrons to the Au adislands. Cr ions in MgO, on the other hand, are stable only in the +2 and +3 charge states and can provide a single electron at best. Since this electron is likely to be captured by cationic vacancies or morphological defects in the real oxide, no charge transfer to Au particles takes place in this case. On the basis of our findings, we have developed general rules on how to optimize the electron donor characteristics of doped oxide materials.

Doping has proven to be a powerful approach for tailoring fundamental properties of oxide materials, including their electronic structure^{1–3} and chemical characteristic.^{4–8} The method relies on the ability of the dopants to exchange electrons with the oxide host and with surface-bound adsorbates. While in the first case, hot electrons/holes are generated in the oxide bands that alter the band alignment, optical properties, and conductivity of the material, the electron transfer triggered in the second scenario may initiate molecular dissociation and reaction events. Controlling such charge-transfer processes into adsorbates via doping is therefore a prime research field in heterogeneous catalysis. Indeed, the reactivity of various oxides was found to increase upon doping, as demonstrated for instance for the activation of methane over Li-doped MgO⁷ and the oxidation of CO on TiO₂ loaded with transition metal (TM) impurities.⁸ Moreover, doping was identified as a versatile means for tailoring the equilibrium shape and thermodynamic stability of metal particles on oxide supports, which are also decisive parameters in heterogeneous catalysts.^{9–11}

Because of its compelling simplicity, a basic charge-transfer picture is often consulted to describe the role of impurity ions in a host lattice, although it often fails to capture the complexity of the real system. Especially in oxide materials, dozens of

mechanisms that suppress or modify the anticipated electron exchange are at work. For example, hole states generated by undervalent cationic impurities are often annihilated by an equal amount of charged O vacancies (e.g., F⁺ color centers)¹² or by adsorbing donor molecules (e.g., hydrogen).¹³ Conversely, the excess electrons released by overvalent dopants may be captured by structural inhomogeneities in the oxide lattice (e.g., by grain boundaries).¹⁴ In addition, whether the desired charge transfer takes place depends on the energy position of the donor (acceptor) level with respect to the affinity state of the adsorbate. Reliable prediction of the dopant's ability to act as an electron donor or acceptor in a given host oxide therefore requires a careful analysis of every single case.

In this work, we present two model systems for doped oxide materials that have isostructural and isoelectronic properties and still behave entirely differently. The two group 6 metals Cr and Mo were used as dopants, as they exhibit similar electronic structures [*ns*¹(*n* – 1)*d*⁴] and ionization energies. They were inserted into the two rock salt oxides MgO and CaO, respectively, both of which are wide-gap insulators with band gaps of >7.0 eV. We selected these two host oxides because they enabled rather strain-free embedding of the TM impurities. While Cr³⁺ ions (75 pm) are of similar size as the substituted Mg²⁺ (71 pm), Mo³⁺ (87 pm) fits well into Ca²⁺ substitutional sites (99 pm).¹⁵ The residual mismatch in the case of CaOMo leads to a local inward relaxation of O ions in the first coordination shell of the dopant that amounts to ~0.2 Å (see the Supporting Information). We note that CaO with its larger lattice parameter has also a smaller Madelung potential and is therefore more reactive than MgO.

The doped oxide systems were prepared as thin films via Mg (Ca) deposition onto sputtered and annealed Mo(001) single crystals in oxygen at a pressure of 5 × 10^{–7} mbar.^{16,17} The dopants were introduced by adding 1 atom % Cr (Mo) to the gas vapor used for the oxide growth. The film thickness was adjusted to 20 (60) monolayers (ML) for MgO_{Cr} (CaO_{Mo}) to suppress interface effects induced by the Mo(001) support. These values correspond to the maximum thicknesses that can still be probed with scanning tunneling microscopy (STM), a technique that relies on a finite conductivity of the oxide films. Surface segregation of the dopants was suppressed by growing five pristine oxide layers on top of the doped films. After

Received: May 9, 2012

Published: June 28, 2012



annealing to 1000 K, a sharp (1×1) square pattern corresponding to a rock salt (001) surface was observed by low-energy electron diffraction (LEED), while STM images of the films revealed large, atomically flat terraces separated by mainly [100]-oriented dislocation lines (Figure 1). Although no dopant signature was detected by STM and LEED, their presence could be verified by means of Auger spectroscopy and, for MgO_{Cr} , cathodoluminescence spectroscopy.¹⁸

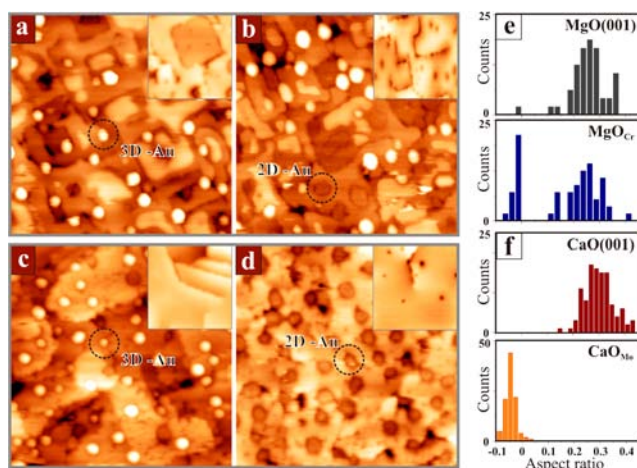


Figure 1. (a, b) STM topographic images of (a) bare and (b) Cr-doped $\text{MgO}(001)$ films with a thickness of 20 ML after dosing of 0.5 ML Au ($60 \text{ nm} \times 50 \text{ nm}$, 5.5 V). The insets display the respective surfaces before Au deposition ($20 \text{ nm} \times 20 \text{ nm}$). (c, d) Similar measurements on (c) bare and (d) Mo-doped $\text{CaO}(001)$ with a thickness of 60 ML ($60 \text{ nm} \times 60 \text{ nm}$, 6.0 V). The 2D Au islands appear as faint depressions on both surfaces, because electron transport from the STM tip into the surface is inhibited upshifted field-emission resonances above the Au islands.¹⁹ (e, f) Histograms of the particle aspect ratios (height/diameter) measured on the pristine and doped oxide films. The negative apparent height of the 2D gold in the images gives rise to negative aspect ratios in the histogram.

Charge transfer processes involving the TM dopants were identified by depositing 0.5 ML Au on top of the CaO_{Mo} and MgO_{Cr} films at room temperature. The equilibrium geometry of Au particles is known to be sensitive to their charge state.^{20,21} Whereas neutral particles adopt compact three-dimensional (3D) shapes because of the small energy gain from interfacial interactions with the oxide support, two-dimensional (2D) islands form in the presence of excess electrons in the gold. This crossover in particle geometry is driven by effective electrostatic and polaronic interactions between Au^- and the oxide lattice²² and results in a spreading of the metal on the oxide support. Indeed, the equilibrium shape of the Au deposits was found to change upon doping of the MgO and CaO films (Figure 1). While Au grew into 3D deposits on the pristine oxides, monolayer islands developed on CaO_{Mo} films. Surprisingly, no geometry crossover was observed for MgO_{Cr} where the vast majority of particles retained a 3D configuration and only few aggregates adopted a 2D shape. The difference became evident in shape histograms obtained by plotting the aspect ratios (height/diameter) of ~ 500 Au particles observed on the different substrates (Figure 1e,f). The dimensionality change affected 100% of the Au particles on CaO_{Mo} but was limited to a small number of deposits on MgO_{Cr} . Apparently, only Mo dopants are able to donate electrons into the admetal, while Cr is electrically inactive [see the X-ray photoelectron

spectra in the Supporting Information for additional proof]. In view of the similar electronic properties of the two TM ions, the question arises why Mo is a better dopant than Cr.

To elucidate the difference between the two doped oxides, we analyzed their electronic structures and the binding properties of gold by means of density functional theory (DFT). The calculations were performed with the projector-augmented plane-wave method (400 eV energy cutoff) and the Perdew–Burke–Ernzerhof (PBE) functional as implemented in the Vienna Ab Initio Simulation Package.²³ Some key results were verified with hybrid functional (PBE0) calculations. The films were modeled with a five-layer-thick (3×3) surface cell with one impurity ion substituting for a cation in the center of the slab and one Au atom being adsorbed to its surface. The Brillouin zone was sampled with a ($2 \times 2 \times 1$) k -point mesh. Formation energies of cationic vacancies (V_{M} defects), referred to the respective bulk metals, were determined with Γ -point calculations on a ($3 \times 3 \times 3$) unit cell containing 108 MO units ($M = \text{Mg}, \text{Ca}$). Different charge states of the dopants were considered by using a compensating background charge density.²⁴ We carefully checked that this method did not introduce artifacts in the calculations, as we compared results obtained for charged and neutral supercells. In the latter case, charged TM ions were generated by introducing compensating defects.

In a neutral nondefective slab, the Cr (Mo) ions adopt a formal 2+ charge state, reflecting the nature of the substituted Mg (Ca) species. The respective electron configurations are $t_{2g}^3 e_g^1$ for Cr^{2+} and t_{2g}^4 for Mo^{2+} in a bulk environment, but the latter changes to a high-spin $t_{2g}^3 e_g^1$ configuration for Mo^{2+} in a near-surface region. In any case, electron transfer to the host material is inhibited by the high energy of the oxide conduction bands. The situation changes when a Au atom is adsorbed onto the surface. As the initially half-filled Au 6s orbital is now lower in energy than the highest occupied dopant level, the Au atom accepts one TM d electron, and its affinity level becomes doubly occupied (Figure 2). The charge transfer becomes evident from the calculated Bader charge of the Au atom, which increases from $-0.3e$ to $-0.8e$ upon doping. Because of this

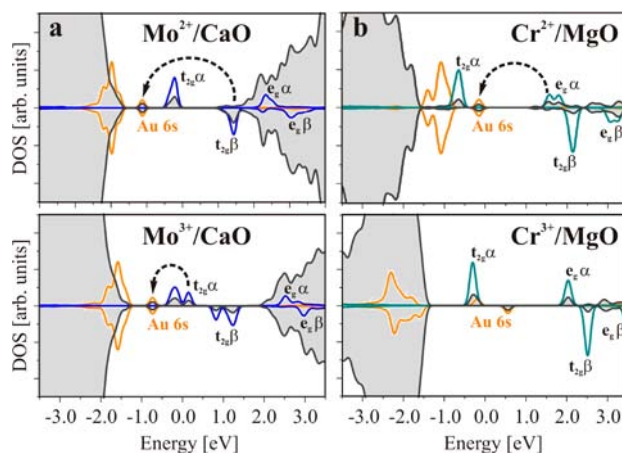


Figure 2. Projected densities of states (DOS) for (a) CaO_{Mo} and (b) MgO_{Cr} in the presence of a Au atom calculated for two different charge states of the TM ion. The DOS was obtained for the most stable configuration of each system (O-top for $\text{Cr}^{3+}/\text{MgO}$, hollow sites otherwise) and aligned to the highest occupied state. Charge transfers from the HOMO of the dopant to the Au 6s affinity levels are indicated by arrows.

change in charge state, the binding energy of the Au atom rises from 1.03 (1.35) eV on the bare MgO (CaO) surface to 2.97 (3.60) eV on the Cr (Mo)-doped film. Simultaneously, the preferred binding position moves from an O-top site to a hollow site, though adjacent Mg and O sites offer similar binding strengths as a result of an effective polarization of the oxide lattice.²⁵ Apparently, both Cr²⁺ and Mo²⁺ act as charge donors and would induce a 3D/2D crossover in the growth morphology of gold, in contrast to the experimental findings.

In real systems, electron traps that provoke a spontaneous charge drain from the impurity ion to the defect might be present.^{14,26} The existence of overvalent dopants, for example, is known to increase the number of V_M defects in the oxide lattice, as demonstrated by paramagnetic resonance and optical spectroscopy.^{27,28} Each V_M center produces two holes in the 2p states of nearby O ions that are filled by the high-lying d electrons of the TM impurity, according to the reaction $2TM^{2+} + V_M + 2O^{2-} \rightarrow 2TM^{3+} + V_M + 2O^{2-}$. By this means, energetically unfavorable defect states in the band gap are emptied, and the total energy of the system becomes lower. Our DFT calculations revealed that the formation energy of a V_M defect in the presence of two TM dopants decreases from ~8 eV in the two stoichiometric oxides to 0.97 (1.68) eV in the MgO_{Cr} (CaO_{Mo}) system. The formation of V_M defects is thus expected to occur in our doped oxides, especially as the films are annealed to 1000 K during preparation. The STM topographies indeed displayed atom-sized depressions in the oxide surface, the density of which scaled with the dopant concentration (Figure 1, insets).¹⁸ Moreover, the surface density of those vacancies was found to be higher in MgO than in CaO films at similar doping levels, reflecting the higher V_M formation energy in the latter case. We abstain from a quantitative discussion of measured defect densities at this point, as we have no information on the bulk concentration of the cationic vacancies. Moreover, additional electron traps are known to be present along the dislocation lines of the MgO and CaO films.²⁶ It should be noted that the occurrence of dopant-induced surface defects may alter the Au nucleation behavior but cannot explain the observed switch in particle shape that requires an overall change in the metal–oxide adhesion.

To account for the existence of intrinsic charge traps in MgO and CaO films, we calculated the Au binding behavior for a scenario in which the dopant had already lost an electron to a parasitic acceptor state. A Mo³⁺ ion in CaO_{Mo} is still able to donate an electron to a surface Au atom, which subsequently experiences a bond reinforcement (2.10 eV). Even Mo⁴⁺ may act as a charge donor, although the electron transfer is energetically less favorable in this case and the Au binding energy drops to 1.72 eV, compared with 1.35 eV without doping. A different situation was found for MgO_{Cr}, where already the Cr³⁺ species cannot be oxidized any further, and the charge transfer toward gold ceases. The evolution of the donor strength with increasing oxidation state is reflected in the position of highest occupied d state (HOMO) of the dopant relative to the Au 6s affinity level. The t_{2g} donor level of Mo progressively shifts downward in the band gap as Mo goes from the +2 to the +3 and +4 charge state, reducing the energy gain associated with an electron transfer into the Au (Figure 2). In contrast, while the HOMO of Cr²⁺ is still above the Au 6s position, the Cr³⁺ HOMO drops below the Au affinity level, which renders any electron transfer impossible. Evidently, charge donation into Au atoms is a robust effect for Mo

impurities even in the presence of parasitic electron traps but occurs only in an ideal, defect-free oxide environment for Cr.

The fundamental reason for the different characteristics of MgO_{Cr} and CaO_{Mo} lies in the nature of the dopant rather than in the oxide properties. Analysis of the Au interaction with the two hypothetical systems MgO_{Mo} and CaO_{Cr} revealed that Mo³⁺ in MgO can still be oxidized to Mo⁴⁺ by donation of an electron to gold, while Cr³⁺ remains electrically inactive also in CaO and no charge transfer takes place.²⁹ In simple terms, this difference reflects the 3 eV higher ionization energy of Cr³⁺ relative to Mo³⁺ and is thus an atomic property of the TM ions. However, the oxide matrix also has an effect. While Mo³⁺ acts as a charge donor in both matrices, the energy gain is smaller and the Au atom binding weaker for MgO_{Mo} (1.20 eV) than for CaO_{Mo} (2.10 eV). According to crystal field theory,²⁸ the larger lattice parameter of CaO reduces the stabilization of the t_{2g} levels and pushes the Mo³⁺ states to higher energies, which in turn makes the TM ions better charge donors than in the spatially contracted MgO lattice.

In conclusion, we have shown that TM dopants may exhibit rather different abilities to transfer charges into adsorbates, even if they belong to the same group in the periodic table. The ability of heavy TM atoms to assume higher oxidation states was found to be important in producing potential electron donors. Also, a large lattice parameter of the host oxide is beneficial for a robust donor characteristic, as this reduces the coupling of the TM impurity to its environment and shifts its HOMO level to higher energy inside the gap. We therefore propose that incorporating second- or third-series TM ions into spacious oxide lattices is a reliable route to produce systems with good donor characteristics.

■ ASSOCIATED CONTENT

📄 Supporting Information

XPS spectra of Mo-doped CaO and a structure model for CaO_{Mo} visualizing the local lattice distortion induced by the dopants. This material is available free of charge via the Internet at <http://pubs.acs.org>.

■ AUTHOR INFORMATION

Corresponding Author

nilius@fhi-berlin.mpg.de; livia.giordano@mater.unimib.it

Author Contributions

§F.S. and X.S. contributed equally.

Notes

The authors declare no competing financial interest.

■ ACKNOWLEDGMENTS

F.S. is grateful for financial support from the Alexander von Humboldt Foundation. The authors acknowledge support from the DFG Excellence Initiative “Unicat” and the Italian MIUR through the FIRB Project RBAP115AYN and thank the Regione Lombardia (LISA) and CILEA for a CPU Grant.

■ REFERENCES

- (1) Janisch, R.; Gopal, P.; Spaldin, N. A. *J. Phys.: Condens. Matter* **2005**, *17*, R657–R689.
- (2) Asahi, R.; Morikawa, T.; Ohwaki, T.; Aoki, K.; Taga, Y. *Science* **2001**, *293*, 269–271.
- (3) Zheng, H.; Kröger, J.; Berndt, R. *Phys. Rev. Lett.* **2012**, *108*, No. 076801.
- (4) (a) Rodriguez, J. A.; Hanson, J. C.; Kim, J. Y.; Liu, G.; Iglesias-Juez, A.; Fernandez-Garcia, M. *J. Phys. Chem. B* **2003**, *107*, 3535–3543.

- (b) Nambu, A.; Graciani, J.; Rodriguez, J. A.; Wu, Q.; Fujita, E.; Sanz, J. F. *J. Chem. Phys.* **2006**, *125*, No. 094706.
- (5) Shapovalov, V.; Metiu, H. *J. Catal.* **2007**, *245*, 205–214.
- (6) Metiu, H.; Chretien, S.; Hu, Z.; Li, B.; Sun, X. Y. *J. Phys. Chem. C* **2012**, *116*, 10439–10450.
- (7) (a) Wang, J. X.; Lunsford, J. H. *J. Phys. Chem.* **1986**, *90*, 5883–5887. (b) Ito, T.; Wang, J. X.; Lin, C. H.; Lunsford, J. H. *J. Am. Chem. Soc.* **1985**, *107*, 5062–5068.
- (8) Kim, H. Y.; Lee, H. M.; Ganesh, R.; Pala, S.; Shapovalov, V.; Metiu, H. *J. Phys. Chem. C* **2008**, *112*, 12398–12408.
- (9) Martinez, U.; Jerratsch, J.-F.; Nilius, N.; Giordano, L.; Pacchioni, G.; Freund, H.-J. *Phys. Rev. Lett.* **2009**, *103*, No. 056801.
- (10) Mammen, N.; Narasimhan, S.; de Gironcoli, S. *J. Am. Chem. Soc.* **2011**, *133*, 2801–2803.
- (11) (a) Shao, X.; Prada, S.; Giordano, L.; Pacchioni, G.; Nilius, N.; Freund, H.-J. *Angew. Chem., Int. Ed.* **2011**, *50*, 11525–11527. (b) Shao, X.; Nilius, N.; Freund, H.-J. *J. Am. Chem. Soc.* **2012**, *134*, 2532–2534.
- (12) Myrach, P.; Nilius, N.; Levchenko, S. V.; Gonchar, A.; Risse, T.; Dinse, K.-P.; Boatner, L. A.; Frandsen, W.; Horn, R.; Freund, H.-J.; Schlögl, R.; Scheffler, M. *ChemCatChem* **2010**, *2*, 854–862.
- (13) Hu, Z.; Li, B.; Sun, X. Y.; Metiu, H. *J. Phys. Chem. C* **2011**, *115*, 3065–3074.
- (14) McKenna, K. P.; Shluger, A. L. *Nat. Mater.* **2008**, *7*, 859–862.
- (15) *CRC Handbook of Chemistry and Physics*; Lide, D. R., Ed.; CRC Press: Boca Raton, FL, 2010.
- (16) Benedetti, S.; Benia, H. M.; Valeri, S.; Freund, H.-J. *Chem. Phys. Lett.* **2006**, *430*, 330–335.
- (17) Shao, X.; Myrach, P.; Nilius, N.; Freund, H.-J. *J. Phys. Chem. C* **2011**, *115*, 8784–8789.
- (18) Stavale, F.; Nilius, N.; Freund, H.-J. *New J. Phys.* **2012**, *14*, No. 033006.
- (19) Ricci, D.; Bongiorno, A.; Pacchioni, G.; Landman, U. *Phys. Rev. Lett.* **2006**, *97*, No. 036106.
- (20) Sterrer, M.; Risse, T.; Heyde, M.; Rust, H.-P.; Freund, H.-J. *Phys. Rev. Lett.* **2007**, *98*, No. 206103.
- (21) Pacchioni, G.; Giordano, L.; Baistrocchi, M. *Phys. Rev. Lett.* **2005**, *94*, No. 226104.
- (22) Shao, X.; Nilius, N.; Freund, H.-J. *Phys. Rev. B* **2012**, *85*, No. 115444.
- (23) (a) Kresse, G.; Hafner, J. *Phys. Rev. B* **1993**, *47*, R558–R561. (b) Kresse, G.; Furthmüller, J. *Phys. Rev. B* **1996**, *54*, 11169–11186.
- (24) Leslie, M.; Gillan, M. J. *J. Phys. C: Solid State Phys.* **1985**, *18*, 973–982.
- (25) Giordano, L.; Pacchioni, G. *Acc. Chem. Res.* **2011**, *44*, 1244–1252.
- (26) Benia, H. M.; Myrach, P.; Gonchar, A.; Risse, T.; Nilius, N.; Freund, H.-J. *Phys. Rev. B* **2010**, *81*, No. 241415R.
- (27) Carroll, J. C. G.; Corish, J.; Henderson, B.; Mackrodt, W. C. *J. Mater. Sci.* **1988**, *23*, 2824–2836.
- (28) Henderson, B.; Imbusch, G. F. *Optical Spectroscopy of Inorganic Solids*; Clarendon Press: Oxford, U.K., 1989.
- (29) The occurrence of charge transfer was deduced from the Bader charges and the magnetic moments. For MgO_{Mol} , the Au Bader charge amounts to $-0.7e$, and two unpaired electrons are localized in the Mo, while no magnetization is left on the Au. For CaO_{Cr} , the Au Bader charge is $-0.3e$, and the system is in a quintet spin state with one unpaired electron on the Au and three on the Cr.